Eur J Nucl Med Mol Imaging (2010) 37:49–57
DOI 10.1007/s00259-009-1204-z

ORIGINAL ARTICLE

# Comparison of $^{68}$Ga-DOTATATE and $^{18}$F-fluorodeoxyglucose PET/CT in the detection of recurrent medullary thyroid carcinoma

**Brendon G. Conry · Nikolaos D. Papathanasiou · Vineet Prakash · Irfan Kayani · Martyn Caplin · Shahid Mahmood · Jamshed B. Bomanji**

Received: 13 May 2009 / Accepted: 9 June 2009 / Published online: 7 August 2009


**Abstract**
*Purpose* This was a retrospective study to detect and map the extent of disease in recurrent medullary thyroid carcinoma (MTC) using the novel PET somatostatin analogue $^{68}$Ga-DOTATATE and conventional $^{18}$F-FDG positron emission tomography/computed tomography (PET/CT).
*Methods* Eighteen patients (13 men, 5 women, median age: 54 years) who had previously been operated on for MTC and presented with biochemical (raised calcitonin levels) and/or imaging evidence of recurrence underwent both $^{68}$Ga-DOTATATE and $^{18}$F-FDG PET/CT within a maximum interval of 4 weeks (median interval of 1 week). $^{68}$Ga-DOTATATE- and $^{18}$F-FDG-avid lesions were recorded per patient as well as per region in six distinct regions: (1) thyroid bed—local recurrence, (2) cervical lymph nodes, (3) mediastinum, (4) lungs, (5) liver and (6) bones. The $^{68}$Ga-DOTATATE and $^{18}$F-FDG PET/CT findings were classified as positive or negative on visual interpretation. These findings were further characterised as concordant or discordant, depending on whether there was agreement or discrepancy in imaging with the two radiotracers. A separate analysis of the unenhanced CT component of the examination was performed. Verification of the lesions was achieved by histopathological analysis, further imaging studies and clinical follow-up.
*Results* $^{68}$Ga-DOTATATE PET/CT imaging achieved disease detection in 13 of 18 and $^{18}$F-FDG PET/CT in 14 of 18 patients. These results corresponded to per-patient sensitivities of 72.2% [95% confidence interval (CI): 46.4–89.3%] for $^{68}$Ga-DOTATATE versus 77.8% (95% CI: 51.9–92.6%) for $^{18}$F-FDG (non-significant difference). $^{18}$F-FDG revealed a total of 28 metastatic MTC regions and $^{68}$Ga-DOTATATE 23 regions. In ten patients a discordant tracer pattern of per-region and/or per-lesion distribution of recurrent disease was observed, while in four patients a concordant pattern was noted (no lesions were detected by either modality in the remaining four patients).
*Conclusion* Neither $^{18}$F-FDG nor $^{68}$Ga-DOTATATE PET/CT can fully map the extent of disease in patients with recurrent MTC, although $^{18}$F-FDG PET/CT may identify more lesions. However, $^{68}$Ga-DOTATATE PET/CT can be a useful complementary imaging tool and may identify patients suitable for consideration of targeted radionuclide somatostatin analogue therapy.

**Keywords** Medullary thyroid carcinoma · Positron emission tomography · $^{18}$F-fluorodeoxyglucose · $^{68}$Ga-DOTATATE

An Editorial Commentary on this paper is available at http://dx.doi.org/10.1007/s00259-009-1247-1

N. D. Papathanasiou · V. Prakash · I. Kayani · J. B. Bomanji (✉)
Institute of Nuclear Medicine, University College Hospital,
235 Euston Road,
London NW1 2BU, UK
e-mail: jamshed.bomanji@uclh.nhs.uk

B. G. Conry
Department of Radiology and Nuclear Medicine,
Pembury Hospital,
Tunbridge Wells, UK

M. Caplin
Department of Gastroenterology, Royal Free Hospital,
London, UK

S. Mahmood
Singapore PET and Cardiac Imaging Centre,
Singapore 238859, Singapore

## Introduction

Medullary thyroid carcinoma (MTC) is a rare tumour accounting for 3–5% of all thyroid malignancies. MTC metastasises early to cervical lymph nodes (55–75% of cases), mainly in the central compartment of the neck [1–3]. Distant metastases of MTC are detected in 10–15% of patients at initial presentation and typically occur in the mediastinum, lungs, liver and bone [1, 4]. Serum calcitonin (Ct) is the most accurate hormonal tumour marker of MTC for initial diagnosis, monitoring the effects of treatment and detection of recurrent disease [4, 5]. Total thyroidectomy with extensive neck dissection is the only effective curative treatment, targeting the removal of the entire neoplastic burden [2, 6]. Even after such aggressive surgery, 40% of patients have persistent disease, as indicated by measurable Ct levels, while another 10% with undetectable postoperative Ct will later develop tumour recurrence [4, 7]. The early detection of residual/recurrent tumour and the accurate evaluation of the extent of disease are crucial steps in therapeutic management, with a view to curative surgery as the primary treatment strategy. Systemic treatment modalities (radiotherapy, chemotherapy, tyrosine kinase inhibitors and radionuclide therapy) are applied, albeit with limited success in extensive metastatic disease [6, 8].

Numerous imaging techniques have been used to detect recurrent MTC. Morphological cross-sectional imaging methods (neck ultrasound, CT, MRI) as well as scintigraphic imaging techniques with planar and single photon emission computed tomography (SPECT) acquisitions and the use of different radiotracers (pentavalent DMSA, $^{123}$I-MIBG and $^{111}$In-octreotide) have been only partly successful in this context. In particular, the latter demonstrated less than satisfactory sensitivity [6, 9, 10] owing to inherently poor spatial resolution and lack of anatomical corroboration. The advent of positron emission tomography/computed tomography (PET/CT) brought about dramatic improvements in image spatial resolution and anatomical lesion localisation. The vast majority of PET oncology studies are being performed with $^{18}$F-FDG, a glucose analogue, which has been successfully used to detect malignant cells with increased glucose metabolism. Though established as an imaging standard for many cancer types [11] with increased glycolytic load, $^{18}$F-FDG has produced suboptimal results in MTC patients and a considerable number of false-negative studies, especially in patients with low Ct levels [12].

Owing to their neuroendocrine origin and behaviour, MTC cells express somatostatin receptors on their surface. In vitro reverse transcriptase polymerase chain reaction (RT-PCR) studies, in MTC cell lines, have identified somatostatin receptor 2 (SSTR2) and 5 (SSTR5) as the most frequent subtypes expressed in this tumour [13, 14]; however, immunohistochemical studies have produced generally low estimates for SSTR density [15]. In vivo detection of SSTR expression has, so far, been the molecular basis for tumour imaging with radiolabelled somatostatin analogues in SPECT imaging, such as $^{111}$In-octreotide. $^{68}$Ga-DOTATATE is a novel PET tracer which consists of DOTA-DPhe$^{1}$,Tyr$^{3}$-octreotate (DOTATATE), an SSTR2 analogue labelled with $^{68}$Ga, a generator-derived positron emitter isotope (half-life 68 min). $^{68}$Ga-DOTATATE has high affinity for SSTR2 [16], demonstrates fine target to non-target imaging properties and has already shown satisfactory sensitivity in neuroendocrine tumour imaging [17]. Thus prompted, we tried to investigate $^{68}$Ga-DOTATATE's diagnostic performance in the detection of recurrent MTC. Moreover we performed direct comparisons of the utility of $^{68}$Ga-DOTATATE and $^{18}$F-FDG in these patients; the added value of the unenhanced CT component of the PET/CT examination was also evaluated. In this way, we attempted to detect and map the whole tumour burden by exploiting two distinct features at the cellular level, namely somatostatin receptor expression and glucose metabolism. We also attempted to reveal probable clinical implications of combined $^{68}$Ga-DOTATATE and $^{18}$F-FDG imaging, e.g. with respect to staging, correlations with tumour markers, clinical decision making or selection of candidate patients for radionuclide therapy.

## Materials and methods

The retrospective analysis included 18 patients (13 men, 5 women, age range: 34–75 years, median age: 54 years) with recurrent histologically proven sporadic MTC, who had contemporaneous $^{18}$F-FDG and $^{68}$Ga-DOTATATE PET/CT imaging tests from September 2005 to December 2008. Informed consent was obtained from all patients prior to imaging studies. Studies had been performed in two centres: the Institute of Nuclear Medicine, University College Hospital, London and the Singapore PET and Cardiac Imaging Centre, Singapore. PET/CT imaging was performed either:

(a) For the detection of occult disease in cases of raised Ct levels (patients 13–18, Table 1)—in these cases previous conventional imaging tests (ultrasound, CT) were negative or inconclusive—or
(b) For the assessment of the extent of residual, recurrent or metastatic disease (patients 1–12) suggested by clinical examination or other imaging modalities. The interval between the two studies ranged from 0 to 4 weeks (median interval 1 week), which was considered sufficiently short for a relatively slowly progressive tumour such as MTC.

**Table 1** Imaging results of the patients of the study. Involved regions and corresponding number of positive $^{18}$F-FDG and $^{68}$Ga-DOTATATE lesions are presented for each patient. The positive findings of the independent reading of the unenhanced CT data are shown. Recent calcitonin levels and maximum standardised uptake values ($SUV_{max}$) of the uptake of $^{18}$F-FDG and $^{68}$Ga-DOTATATE in the corresponding positive lesions with the greatest tracer accumulation are displayed

| Patient No./ age/ sex | Serum calcitonin (pg/ml) | Positive region(s) | $^{18}$F-FDG | $^{68}$Ga-DOTATATE | Unenhanced CT | Comparison of $^{18}$F-FDG and $^{68}$Ga-DOTATATE | $SUV_{max}$ for $^{18}$F-FDG, respective lesion | $SUV_{max}$ for $^{68}$Ga-DOTATATE, respective lesion |
|---|---|---|---|---|---|---|---|---|
| 1/65/M | 7,500 | Neck nodes | 2 | 0 | 0 | Discordant | 7.7, iliac bone | 4.6, sacrum |
| | | Bone | 8 | 5 | 2 | | | |
| 2/53/M | 1,500 | Neck nodes | 2 | 2 | 1 | Discordant | 4.4, liver | 16.9, liver |
| | | Liver | 1 | 2 | 0 | | | |
| 3/37/F | 107 | Thyroid bed | 2 | 2 | 2 | Discordant | 7.8, iliac bone | 6.0, iliac bone |
| | | Neck nodes | 2 | 2 | 2 | | | |
| | | Hila | 3 | 3 | 3 | | | |
| | | Lung | 1 | 0 | Extensive disease | | | |
| | | Liver | 3 | 0 | | | | |
| | | Bone | Extensive disease/ superior | Extensive disease | Extensive disease | | | |
| 4/75/M | 15,600 | Neck nodes | 1 | 1 | 0 | Discordant | 7.9, neck node | 7.4, vertebra |
| | | Liver | 4 | 0 | 0 | | | |
| | | Bone | 5 | 5 | 3 | | | |
| 5/44/F | 5,340 | Thyroid bed | 1 | 1 | 1 | Discordant | 4.9, thyroid bed | 8.6, thyroid bed |
| | | Neck nodes | 3 | 3 | 3 | | | |
| | | Mediastinum | 2 | 3 | 3 | | | |
| 6/58/M | 59 | Bone | 3 | 3 | 3 | Concordant | 8.3, sternum | 9.7, sternum |
| 7/70/M | 133 | Thyroid bed | 1 | 0 | | Discordant | 4.6, thyroid bed | |
| 8/50/M | 256 | Thyroid Bed | 1 | 1 | 1 | Concordant | 14.0, thyroid bed | 9.1, thyroid bed |
| | | Neck nodes | 3 | 3 | 2 | | | |
| 9/60/F | 550 | Bone | Extensive disease | Extensive disease/ superior | Extensive disease | Discordant | 5.6, vertebra | 8.1, vertebra |
| 10/60/M | 176 | Neck nodes | 1 | 1 | 1 | Discordant | 6.0, vertebra | 8.4, vertebra |
| | | Bone | 6 | 4 | 4 | | | |
| 11/50/F | 56 | Neck nodes | 3 | 3 | 2 | Discordant | 5.2, neck node | 5.1, neck node |
| | | Lung | 5 | 3 | 3 | | | |
| 12/40/M | 241 | Bone | 6 | 5 | 4 | Discordant | 4.4, rib | 7.3, sacrum |
| 13/47/F | 51 | None | 0 | 0 | 0 | Concordant | | |
| 14/66/M | 38 | None | 0 | 0 | 0 | Concordant | | |
| 15/34/M | 350 | Thyroid bed | 1 | 1 | 1 | Concordant | 4.3, thyroid bed | 4.5, thyroid bed |
| 16/55/M | n.a. | None | 0 | 0 | 0 | Concordant | | |
| 17/53/M | 46 | Neck nodes | 2 | 2 | 3 | Concordant | 4.6, neck node | 3.9, neck node |
| 18/56/M | n.a. | None | 0 | 0 | 0 | Concordant | | |

*n.a.*: not available, *extensive disease* >15 lesions, *superior* detected more lesions than the other modalities

All patients had previously undergone total thyroidectomy together with lymph node dissection for MTC. Four of them (patients 1, 2, 7 and 13) had additional neck operations for disease recurrence. Patients' Ct levels were recorded and are presented in Table 1. In all cases the interval between the measurement and PET/CT imaging was less than 1 month.

### $^{68}$Ga –DOTATATE labelling

The commercially available $^{68}$Ge/$^{68}$Ga generator (Eckert & Ziegler, Berlin, Germany and originating from Obninsk, Russia) was washed beforehand with 1.25 ml of 0.1 N ultrapure 30% HCL, while the generator was eluted with 1 ml of 0.1 N HCL. Thus, a high amount of $^{68}$Ga was obtained with minimal $^{68}$Ge breakthrough [15].

Afterwards, an aliquot of 50 ml (~50 mg) DOTATATE (Bachem, Weil am Rhein, Germany) was dissolved in 100 ml of 0.01 N sodium acetate buffer and mixed with 200–800 MBq $^{68}$Ga. The pH of the solution was adjusted to pH 3.5–4 with HCL or sodium acetate buffer as appropriate. The buffered solution was incubated at 95°C for 10 min in a heating block (VWR International, West Chester, PA, USA) and then subjected to sterile filtration using a Millex 0.22 mm filter (Millipore, Billerica, MA, USA). The labelling yield was analysed by instant thin-layer chromatography (ITLC-SG, Pall Inc., Putnam, CT, USA) and HPLC using a Luna 5 mm, C18 (2) 50 × 3.0 mm column (Phenomenex, Torrance, CA, USA) and an acetonitrile-water gradient.

### Imaging protocols

PET/CT studies were performed in the Institute of Nuclear Medicine, University College Hospital using GE Discovery (GE Healthcare, Waukesha, WI, USA) and in the Singapore PET and Cardiac Imaging Centre using Philips Gemini TOF (Philips Healthcare, Best, The Netherlands) dedicated combined PET/CT scanners; whole-body examinations (mid-brain to mid-thigh) were performed with the patient in the supine position. Thirteen patients (1–9 and 13–16) were scanned on the GE scanner and the other five on the Philips Gemini TOF (time of flight) scanner. Since the Philips Gemini TOF is designed for a lower dose of injected tracer, these patients received 195–220 MBq of $^{18}$F-FDG, whereas the patients scanned on the GE scanner with BGO crystal detectors received approximately 370–550 MBq $^{18}$F-FDG. PET/CT images were acquired from 50 to 75 min post-injection on both scanners.

For $^{68}$Ga-DOTATATE PET/CT imaging, 120–220 MBq of activity was administered on the GE scanner, with 90–110 MBq on the Philips TOF scanner. The images were acquired 45–60 min post-injection. No adverse effects were observed after the injection of $^{68}$Ga-DOTATATE; there were no technical problems performing a same-day $^{18}$F-FDG and $^{68}$Ga-DOTATATE PET/CT protocol.

CT data were acquired using the four 3.75-mm detectors, a pitch of 1.5 and a 5-mm collimation on the GE system and 64 0.625-mm detectors, with a pitch of 0.829 and a collimation of 64×0.625 on the Philips system. The CT exposure factors for all examinations were 120–140 kVp and 80 mAs. A separate data set of thoracic CT images was reconstructed with an appropriate algorithm for lung imaging. Maintaining patient position, a whole-body PET emission scan was performed, covering an area identical to that covered by CT. $^{18}$F-FDG PET acquisitions were carried out in 2-D mode (5 min per bed position) on the GE scanner and in 3-D mode (time of flight) on the Philips system (1.5 min per bed position). $^{68}$Ga-DOTATATE PET examinations were acquired in 3-D mode on both scanners, with added TOF technology on the Philips system. PET images were reconstructed using CT for attenuation correction. Transaxial PET emission images of 4.3×4.3×4.25 mm$^3$ were reconstructed using ordered subsets expectation maximisation with 2 iterations and 28 subsets for 2-D mode and 3 iterations and 25 subsets for 3-D mode. The axial field of view was 148.75 mm, resulting in 35 slices per bed position on the GE system. On the Philips system the PET data were acquired in list mode and reconstructed using the time of flight algorithm. The axial field of view for the Philips system was 180 mm, resulting in 36 slices per bed projection.

An experienced nuclear medicine physician (J.B.B.) and a radionuclide radiologist (B.G.C.) reviewed all PET/CT examinations in consensus. Any focus of $^{68}$Ga-DOTATATE or $^{18}$F-FDG superior to background in an unexpected location was interpreted as positive/abnormal. The lesions were recorded per patient as well as per region in six distinct regions: (1) thyroid bed—local recurrence, (2) cervical lymph nodes, (3) mediastinum—hila, (4) lungs, (5) liver and (6) bones. The CT data were independently reviewed by a radionuclide radiologist (B.G.C.) for lesions not visualised on PET imaging. The unenhanced CT was regarded as diagnostic in the evaluation of lung nodules and bone lesions. Multiple lung nodules in a miliary pattern were considered malignant. Bone lesions were characterised as malignant depending on their localisation (involving the vertebral body and/or pedicle) and appearance (osteolysis, cortical destruction or focal sclerosis). Additionally, nodal disease ≥1 cm in the neck, hilar and mediastinal regions was assessed. The conspicuity of these lesions on unenhanced CT was to some extent dependent on the neck and mediastinal fat content, which was variable.

Positive imaging findings were confirmed by one of the following criteria: positive histopathological results from surgical resections or biopsy specimens, presence of a

lesion at the corresponding site on conventional imaging studies or increase in the size of a lesion on follow-up studies. For both ethical and practical reasons, not every lesion interpreted as positive could be evaluated by histology (gold standard). Imaging results were characterised as concordant when there was agreement in lesion identification with both tracers (Fig. 1) and as discordant (Figs. 2 and 3) in cases of discrepancy between $^{68}$Ga-DOTATATE and $^{18}$F-FDG uptake. Sensitivity was calculated for $^{68}$Ga-DOTATATE and $^{18}$F-FDG PET/CT imaging on a per-patient basis. All of the patients in the study were regarded as "positive" for MTC since they had biochemical (raised Ct levels) or previous imaging evidence of disease recurrence. Each patient with at least one verified malignant lesion was counted as "true-positive". The other patients with negative $^{68}$Ga-DOTATATE or $^{18}$F-FDG PET/CT studies were considered as "false-negative".

Semi-quantitative indices (standardised uptake values, SUVs) of the uptake of $^{18}$F-FDG and $^{68}$Ga-DOTATATE were calculated for positive lesions according to the formula $SUV = \frac{Q_l}{Q_{inj}/BW}$, where $Q_l$ = the activity in the lesion in mCi/ml, $Q_{inj}$ = the activity injected in mCi and BW = the patient's body weight in grams. The maximum SUV ($SUV_{max}$) was recorded for each lesion after manually applying regions of interest (ROIs) in the transaxial attenuation-corrected PET slices, around the pixels demonstrating the greatest accumulation of each tracer. Comparisons between SUVs of $^{68}$Ga-DOTATATE and $^{18}$F-FDG have not been performed, since $^{68}$Ga-DOTATATE exhibits totally different pharmacokinetic properties and biodistribution from $^{18}$F-FDG. $^{68}$Ga-DOTATATE uptake represents somatostatin receptor density [17, 18] rather than cell metabolism, so a direct comparison of quantitative measures (SUV) with corresponding $^{18}$F-FDG SUV values would not be straightforward.

## Results

$^{68}$Ga-DOTATATE PET/CT imaging detected at least one site of malignant disease in 13 of 18 patients, while $^{18}$F-FDG PET/CT was positive in 14 of 18 patients. Per-patient analysis demonstrated a sensitivity of 72.2% [95% confidence interval (CI): 46.4–89.3%] for $^{68}$Ga-DOTATATE versus 77.8% (95% CI: 51.9–92.6%) for $^{18}$F-FDG. This difference was not statistically significant (McNemar's test, $p$ value=0.056). There was only one case of per-patient discordance between $^{68}$Ga-DOTATATE and $^{18}$F-FDG; this was in patient 7 with a loco-regional recurrence that demonstrated avidity for $^{18}$F-FDG but not for $^{68}$Ga-DOTATATE. No other patient presented positive results with one tracer and negative results with the other (Table 1). Detection of occult MTC was achieved with both tracers in two of six patients. At least one site of metastatic disease was detected in all 12 patients of the other subgroup who had been evaluated for the extent of residual or recurrent disease.

A total of 55 countable lesions were detected on $^{68}$Ga-DOTATATE and 72 on $^{18}$F-FDG PET/CT. Subsequent per-region analysis revealed 28 regions to be positive on $^{18}$F-FDG PET, compared with 23 on $^{68}$Ga-DOTATATE imaging. Comparisons between tracers revealed four patients (6, 8, 15 and 17) who had a completely concordant pattern of recurrent disease with both tracers; in the other ten patients at least one discordant lesion was recorded. Most of the discrepancies were noted in the liver, lung and skeleton regions. In two patients (3 and 4) (Fig. 2), $^{18}$F-FDG-avid liver metastases were detected which were all negative on $^{68}$Ga-DOTATATE imaging. In contrast, in patient 2 (Fig. 3), $^{68}$Ga-DOTATATE detected two liver lesions, of which one was also positive on $^{18}$F-FDG PET. Discordant bone metastatic disease was noted in five patients with skeletal metastases. This was most notable in patients 3 and 9, who had the greatest tumour load in this

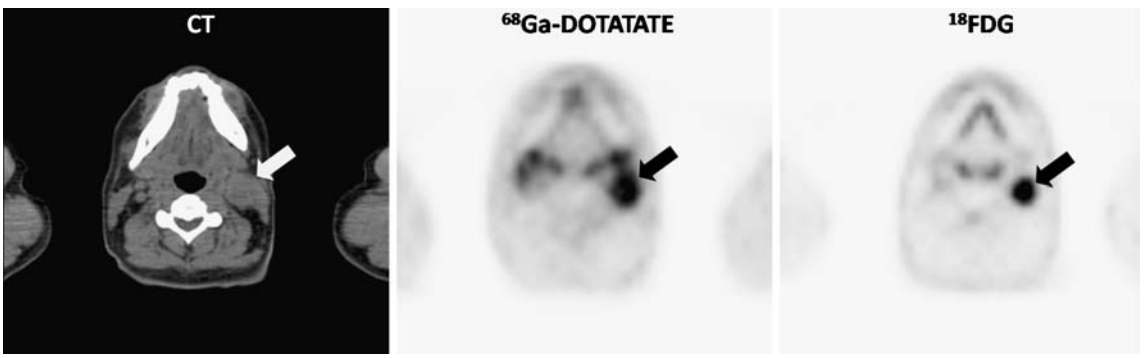


**Fig. 1** Patient 8. Cross-sectional CT (*left panel*), $^{68}$Ga-DOTATATE (*middle panel*) and $^{18}$F-FDG PET (*right panel*) images. There is an enlarged (2.7×2.3 cm) left upper cervical (level II) lymph node (*arrow*) which is avid on both $^{68}$Ga-DOTATATE and $^{18}$F-FDG (concordant lesion)

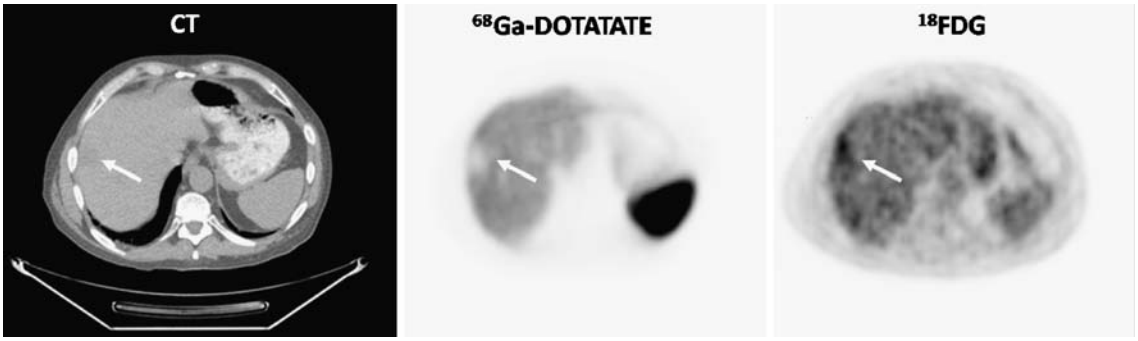


**Fig. 2** Patient 4. Cross-sectional CT (*left panel*), $^{68}$Ga-DOTATATE (*middle panel*) and $^{18}$F-FDG PET (*right panel*) images. An $^{18}$F-FDG-avid liver metastasis (*arrow*) is noted which shows no avidity for $^{68}$Ga-DOTATATE (discordant lesion). Of note, the intense $^{68}$Ga-DOTATATE physiological distribution in the spleen and to a lesser degree in the liver

study and presented with extensive metastatic bone disease. Patient 3 demonstrated a lot more $^{18}$F-FDG-avid bone lesions than $^{68}$Ga-DOTATATE-avid lesions, while the opposite pattern of tracer uptake was noted in patient 9, with bone disease being more avid for $^{68}$Ga-DOTATATE than $^{18}$F-FDG.

In this series, review of the CT data added significant diagnostic information in only one patient: in patient 3, multiple lung nodules were detected; most were very small (<5 mm) and outside the spatial resolution of PET but one in the middle lobe was 16 mm. Bone lesions in our patients could be detected on the CT images, but were more easily and accurately recognised by the use of the radiotracers (either $^{68}$Ga-DOTATATE or $^{18}$F-FDG).

Recent Ct levels (<1 month from PET imaging) were available for 16 of 18 patients (range: 37–15,600 pg/ml, median: 208.5 pg/ml) (Table 1). Though the number of patients was too small to allow for statistical analysis, higher Ct levels generally corresponded to a greater detected tumour burden (higher number of lesions) (Spearman's correlation coefficient $p$ value = 0.034). No correlation was found between SUVs of both tracers and Ct levels (Spearman's correlation coefficient $p$ value = 0.92 for $^{18}$F-FDG and $p$ value = 0.45 for $^{68}$Ga-DOTATATE).

## Discussion

To our knowledge, this is one of the first attempts to detect and map the entire extent of disease in patients with recurrent MTC by the use of the novel PET tracer $^{68}$Ga-DOTATATE. This tracer appeared to be nearly as effective as $^{18}$F-FDG in identifying recurrent MTC. Although calculated sensitivity was marginally less for $^{68}$Ga-DOTATATE than for $^{18}$F-FDG (72.2 vs 77.8%), this difference was not statistically significant. The pattern of tracer uptake seemed to be more or less in accordance with that of $^{18}$F-FDG in a considerable number of regions. The total number of countable lesions detected by $^{18}$F-FDG was higher (72 vs 55), but with the exception of patient 7 there was no overall change in staging between $^{68}$Ga-DOTATATE and $^{18}$F-FDG imaging. In three patients (8, 15 and 17) in whom disease was confined to the neck and curative surgery option could be offered, there was a complete

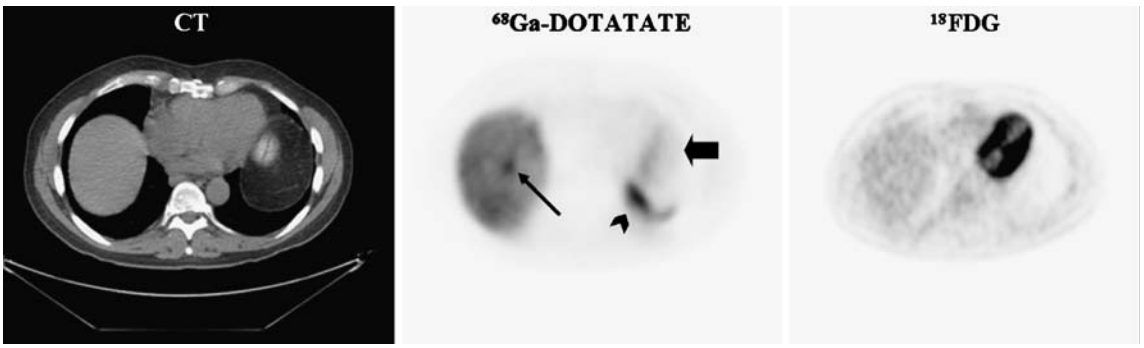


**Fig. 3** Patient 2. Cross-sectional CT (*left panel*), $^{68}$Ga-DOTATATE (*middle panel*) and $^{18}$F-FDG PET (*right panel*) images. There is a metastasis on the liver dome demonstrating avidity for $^{68}$Ga-DOTATATE (*thin arrow*) but not for $^{18}$F-FDG (discordant lesion). Normal uptake pattern of $^{18}$F-FDG in the heart is noted. There is physiological $^{68}$Ga-DOTATATE distribution in the spleen (*arrowhead), the stomach (thick arrow) and the rest of the liver parenchyma*

concordance between the tracers regarding local recurrence and cervical lymph node involvement. In patients 3 and 4 (Fig. 2), $^{68}$Ga-DOTATATE failed to detect the liver lesions which were $^{18}$F-FDG avid but this did not lead to a change in TNM status or clinical management as $^{68}$Ga-DOTATATE had identified bone metastases, leading to classification of these cases as M1 with widespread disease. Interestingly, patient 3, who had predominantly $^{18}$F-FDG-avid bone metastatic disease, had unusually reduced Ct levels relative to the extensive total tumour burden present. In the absence of a Ct assay "hook effect" with high Ct concentrations affecting the binding capacity of the assay antibody, this probably indicates tumour dedifferentiation with some loss of Ct production [19] and a more aggressive tumour behaviour. This might explain the presence of more $^{18}$F-FDG-avid tumour sites, in comparison with $^{68}$Ga-DOTATATE in this patient.

In our study, $^{68}$Ga-DOTATATE demonstrated 72.2% per-patient sensitivity in the detection of biochemically recurrent MTC, which is lower than in the identification of other neuroendocrine tumours [17]. Although somatostatin receptors have been revealed by in vitro studies in MTC cells, they demonstrate a lower incidence and density and a non-homogeneous pattern compared with other endocrine tumours [6, 15]. The clinical significance of somatostatin receptor scintigraphy in MTC is under continuous evaluation. $^{111}$In-octreotide has achieved satisfactory sensitivity for cervical and upper mediastinal lymph nodes in patients with occult MTC, a finding which is typically associated with more benign behaviour, but somatostatin receptor scintigraphy has been suggested to be less sensitive in patients with widespread and progressive disease [20]. Our results seem to contradict this postulate since $^{68}$Ga-DOTATATE somatostatin receptor scintigraphy detected a substantial number of bone and lung lesions in patients with extensive metastatic disease.

In this study, $^{18}$F-FDG PET/CT demonstrated per-patient sensitivity of 77.8% in the detection of recurrent MTC and a low detection rate (33%) of occult MTC, in accordance with previously published results [12, 21]. So far, the calculated sensitivity of $^{18}$F-FDG in this context has fluctuated widely (from 30 to 95%) [9, 10, 12, 21–24]. A large multicentre retrospective German study determined a 78% sensitivity of $^{18}$F-FDG PET in 55 patients with histological confirmation [22], while in the study of Szakall et al., $^{18}$F-FDG PET identified a lot more metastatic MTC lesions (270 lesions) than did CT (141 lesions) or MRI (116 lesions) [23]. However, subsequent studies failed to produce similar results. The prospective study of Giraudet et al. in 55 patients concluded that a combination of imaging methods—neck ultrasound, chest CT, liver and axial skeleton MRI and bone scintigraphy—was the most efficient strategy for depicting MTC tumour sites, whereas $^{18}$F-FDG PET/CT appeared to be less sensitive, identifying tumour lesions in only 58% of the patients [21]. Similar values (sensitivity of 62%) were reported by Ong et al. but with sensitivity increased considerably to the level of 78% in patients with higher Ct levels (>1,000 pg/ml) [12].

The nature and biological behaviour of the tumour can provide a reasonable explanation for the relatively high percentage of false-negative $^{18}$F-FDG PET studies.

MTC, as a well-differentiated neuroendocrine tumour, demonstrates slow rates of progression and low levels of glucose metabolism, with resulting low avidity for $^{18}$F-FDG. This is in accordance with the $^{18}$F-FDG $SUV_{max}$ values calculated for our group of patients (range: 4.3–14, median: 5.4), which were generally low compared with those in other cancer types, even when widespread metastatic disease was present. Musholt et al. have reported that, unlike in other tumours, the expression of transmembrane glucose transporter proteins (GLUT 1–5) is not increased in MTC [25]. Other characteristics of MTC lesions (they are often sclerotic, necrotic or calcified) and their small size, especially in liver and lungs, where they can present with a miliary pattern, offer additional explanations for the suboptimal $^{18}$F-FDG PET sensitivity [21]. Multiple small lung nodules detected in one of our patients (3) appeared negative on both tracers, being below the spatial resolution of the PET imaging system; however, the CT component of the PET/CT examination clearly detected these lesions. With the exception of this patient, the independent reading of the unenhanced CT data did not significantly contribute to mapping the entire extent of the disease. The high contrast inherent in lung CT allows easy detection of sub-centimetre pulmonary nodules. Unenhanced CT was also good at assessing most bony metastases and could visualise some neck and mediastinal nodes but no liver metastases. It is already acknowledged that morphological imaging methods (CT, MRI) are of limited value in the assessment of regional lymph node metastases and local recurrences, especially in the field of postoperative neck changes. Ultrasound-guided fine-needle aspiration biopsy is an efficient method to evaluate loco-regional disease, though its accuracy is operator dependent. It seems that a combination of PET with contrast-enhanced CT would allow whole-body evaluation and the correlation of functional and morphological data, with a consequent probable increase in accuracy in identifying malignant MTC lesions.

Our results show that $^{68}$Ga-DOTATATE detects a significant number of lesions in patients with recurrent MTC without completely delineating the whole tumour burden. In addition, the application of fused PET/CT imaging brings major improvements in spatial resolution and anatomical localisation compared with conventional $^{111}$In-octreotide somatostatin receptor scintigraphy.

$^{68}$Ga-DOTATATE PET/CT may be used as a complementary imaging modality in the detection of recurrent MTC. A potent application of this tracer would be the identification of somatostatin receptor-positive tumour sites, which can be further targeted with radionuclide therapeutic agents, such as $^{90}$Y-DOTATOC or $^{177}$Lu-DOTATATE. This study suggests that many patients, and particularly those with more advanced metastatic disease, would be suitable candidates for such targeted therapies.

Obtaining a more complete tumour biology map of both glycolytic load and SSTR2 density may help to target patients for more aggressive therapy on the basis of the presence of more aggressive MTC. Somatostatin receptor-targeted radionuclide therapy has already shown promising results in gastro-entero-pancreatic (GEP) tumours [26]; however, there is limited experience of these therapeutic agents in MTC [27, 28]. First, Waldherr et al. applied $^{90}$Y-DOTATOC in 12 patients with MTC with poor overall response rates and only some disease stabilisation in patients with clearly progressive disease [28]. Later, another group achieved improved results of $^{90}$Y-DOTATOC therapy in 21 MTC patients, with complete response in 2 (10%), a biochemical response in 6 (28%) and stabilisation of disease in 12 (57%) patients. Patients with a small tumour burden and lower Ct levels had a tendency to respond better [27]. This result suggests a particularly useful imaging indication for $^{68}$Ga-DOTATATE PET/CT, namely the accurate selection of patients who would benefit from earlier application of somatostatin receptor-targeted radionuclide therapy.

**Conflicts of interest** None.

## References


1. Ball DW. Medullary thyroid cancer: monitoring and therapy. Endocrinol Metab Clin North Am 2007;36:823–37. viii.
2. Scollo C, Baudin E, Travagli JP, Caillou B, Bellon N, Leboulleux S, et al. Rationale for central and bilateral lymph node dissection in sporadic and hereditary medullary thyroid cancer. J Clin Endocrinol Metab 2003;88:2070–5.
3. Moley JF, DeBenedetti MK. Patterns of nodal metastases in palpable medullary thyroid carcinoma: recommendations for extent of node dissection. Ann Surg 1999;229:880–7. discussion 887–8.
4. Rufini V, Treglia G, Perotti G, Leccisotti L, Calcagni ML, Rubello D. Role of PET in medullary thyroid carcinoma. Minerva Endocrinol 2008;33:67–73.
5. Elisei R, Bottici V, Luchetti F, Di Coscio G, Romei C, Grasso L, et al. Impact of routine measurement of serum calcitonin on the diagnosis and outcome of medullary thyroid cancer: experience in 10,864 patients with nodular thyroid disorders. J Clin Endocrinol Metab 2004;89:163–8.
6. Rufini V, Castaldi P, Treglia G, Perotti G, Gross MD, Al-Nahhas A, et al. Nuclear medicine procedures in the diagnosis and therapy of medullary thyroid carcinoma. Biomed Pharmacother 2008;62:139–46.
7. Kebebew E, Ituarte PH, Siperstein AE, Duh QY, Clark OH. Medullary thyroid carcinoma: clinical characteristics, treatment, prognostic factors, and a comparison of staging systems. Cancer 2000;88:1139–48.
8. Jiménez C, Hu MI, Gagel RF. Management of medullary thyroid carcinoma. Endocrinol Metab Clin North Am 2008;37:481–96. x-xi.
9. de Groot JW, Links TP, Jager PL, Kahraman T, Plukker JT. Impact of 18F-fluoro-2-deoxy-D-glucose positron emission tomography (FDG-PET) in patients with biochemical evidence of recurrent or residual medullary thyroid cancer. Ann Surg Oncol 2004;11:786–94.
10. Koopmans KP, de Groot JW, Plukker JT, de Vries EG, Kema IP, Sluiter WJ, et al. 18F-dihydroxyphenylalanine PET in patients with biochemical evidence of medullary thyroid cancer: relation to tumor differentiation. J Nucl Med 2008;49:524–31.
11. von Schulthess GK, Steinert HC, Hany TF. Integrated PET/CT: current applications and future directions. Radiology 2006;238:405–22.
12. Ong SC, Schöder H, Patel SG, Tabangay-Lim IM, Doddamane I, Gönen M, et al. Diagnostic accuracy of 18F-FDG PET in restaging patients with medullary thyroid carcinoma and elevated calcitonin levels. J Nucl Med 2007;48:501–7.
13. Zatelli MC, Piccin D, Tagliati F, Bottoni A, Luchin A, Vignali C, et al. Selective activation of somatostatin receptor subtypes differentially modulates secretion and viability in human medullary thyroid carcinoma primary cultures: potential clinical perspectives. J Clin Endocrinol Metab 2006;91:2218–24.
14. Mato E, Matias-Guiu X, Chico A, Webb SM, Cabezas R, Berná L, et al. Somatostatin and somatostatin receptor subtype gene expression in medullary thyroid carcinoma. J Clin Endocrinol Metab 1998;83:2417–20.
15. Papotti M, Kumar U, Volante M, Pecchioni C, Patel YC. Immunohistochemical detection of somatostatin receptor types 1–5 in medullary carcinoma of the thyroid. Clin Endocrinol 2001;54:641–9.
16. Reubi JC, Schar JC, Waser B, Wenger S, Heppeler A, Schmitt JS, et al. Affinity profiles for human somatostatin receptor subtypes SST1-SST5 of somatostatin radiotracers selected for scintigraphic and radiotherapeutic use. Eur J Nucl Med 2000;27:273–82.
17. Kayani I, Bomanji JB, Groves A, Conway G, Gacinovic S, Win T, et al. Functional imaging of neuroendocrine tumors with combined PET/CT using 68Ga-DOTATATE (DOTA-DPhe1, Tyr3-octreotate) and 18F-FDG. Cancer 2008;112:2447–55.
18. Rufini V, Calcagni ML, Baum RP. Imaging of neuroendocrine tumors. Semin Nucl Med 2006;36:228–47.
19. Costante G, Durante C, Francis Z, Schlumberger M, Filetti S. Determination of calcitonin levels in C-cell disease: clinical interest and potential pitfalls. Nat Clin Pract Endocrinol Metab 2009;5:35–44.
20. Behr TM, Becker W. Metabolic and receptor imaging of metastatic medullary thyroid cancer: does anti-CEA and somatostatin-receptor scintigraphy allow for prognostic predictions? Eur J Nucl Med 1999;26:70–1.
21. Giraudet AL, Vanel D, Leboulleux S, Auperin A, Dromain C, Chami L, et al. Imaging medullary thyroid carcinoma with persistent elevated calcitonin levels. J Clin Endocrinol Metab 2007;92:4185–90.
22. Diehl M, Risse JH, Brandt-Mainz K, Dietlein M, Bohuslavizki KH, Matheja P, et al. Fluorine-18 fluorodeoxyglucose positron emission tomography in medullary thyroid cancer: results of a multicentre study. Eur J Nucl Med 2001;28:1671–6.
23. Szakall S Jr, Esik O, Bajzik G, Repa I, Dabasi G, Sinkovics I, et al. 18F-FDG PET detection of lymph node metastases in medullary thyroid carcinoma. J Nucl Med 2002;43:66–71.

24. Iagaru A, Masamed R, Singer PA, Conti PS. Detection of occult medullary thyroid cancer recurrence with 2-deoxy-2-[F-18]fluoro-D-glucose-PET and PET/CT. Mol Imaging Biol 2007;9:72–7.
25. Musholt TJ, Musholt PB, Dehdashti F, Moley JF. Evaluation of fluorodeoxyglucose-positron emission tomographic scanning and its association with glucose transporter expression in medullary thyroid carcinoma and pheochromocytoma: a clinical and molecular study. Surgery 1997;122:1049–60. discussion 1060–1.
26. Van Essen M, Krenning EP, De Jong M, Valkema R, Kwekkeboom DJ. Peptide receptor radionuclide therapy with radiolabelled somatostatin analogues in patients with somatostatin receptor positive tumours. Acta Oncol 2007;46:723–34.
27. Bodei L, Handkiewicz-Junak D, Grana C, Mazzetta C, Rocca P, Bartolomei M, et al. Receptor radionuclide therapy with 90Y-DOTATOC in patients with medullary thyroid carcinomas. Cancer Biother Radiopharm 2004;19:65–71.
28. Waldherr C, Schumacher T, Pless M, Crazzolara A, Maecke HR, Nitzsche EU, et al. Radiopeptide transmitted internal irradiation of non-iodophil thyroid cancer and conventionally untreatable medullary thyroid cancer using [90Y]-DOTA-D-Phe1-Tyr3-octrotide: a pilot study. Nucl Med Commun 2001;22:673–8.